

LPV Active Power Control and Robust Analysis for Wind Turbines

Shu Wang* and Peter Seiler†

*Department of Aerospace Engineering & Mechanics
University of Minnesota, Minneapolis, MN, 55455, USA*

Active power control (APC) refers to a mode of operation where the wind turbine tracks a desired power reference command. It enables wind farms to perform frequency regulation and to provide ancillary services in the energy markets. This paper presents a linear parameter varying (LPV) approach for APC. The multiple-input, multiple-output controller builds upon a previous gain-scheduled design. An LPV controller is designed to coordinate the blade pitch angle and generator torque, which are standard inputs to a utility scale turbine. The objective is to track a given power reference command while also minimizing the structural loads. The controller has parameter dependence on the wind speed and the power output. The LPV approach, in contrast to the previous ad-hoc gain scheduled design, provides (in theory) guarantees on closed-loop stability and performance. This allows the turbine to be operated smoothly anywhere within the power / wind speed envelope. The performance of this LPV design is evaluated using high fidelity simulations. The robustness of the LPV system is analyzed using the theory of integral quadratic constraints.

Nomenclature

| | |
|-----------|---------------------------------|
| v | Wind speed, m/s |
| β | Blade pitch angle, deg |
| τ | Generator torque, $N \cdot m$ |
| λ | Tip speed ratio (TSR), unitless |
| ω | Rotor speed, rad/s |
| p | Generator power, MW |

I. Introduction

As a promising renewable energy, wind power is increasing fast in energy markets all over the world. Though it only accounts for 3% of the electricity produced globally in 2011, the penetration of wind energy is very high in some European countries.¹ In the United States, the amount of wind energy is expected to increase to about 30% by 2020 to 2030.² The power output of wind turbines is variable due to time-varying wind speeds and this may cause unreliable operation of the power grid. This is not a significant issue when wind power is only a small portion of the total electricity generated on the grid. However, to integrate higher levels of variable wind power into the grid it is important for wind turbines to provide active power control (APC).³ APC can be used for the turbine to respond to fluctuations in grid frequency, termed primary response, and to the power curtailment command from transmission system operator, termed secondary response or automatic generation control (AGC).⁴

Traditional wind turbine control systems⁵ do not provide active power control. The power electronics used in variable speed wind turbines decouple the mechanical/inertial turbine dynamics from the power grid. Thus a wind turbine with a traditional control law does not have the inertial response to a grid frequency

*Graduate Student, wang2927@umn.edu

†Assistant Professor, seiler017@umn.edu

event like a conventional coal power generator.⁶ As a result the wind turbine does not participate in the primary response. Moreover, the power output from the turbine fluctuates with variations in wind speed. As a result, new control strategies are being considered to enable wind turbines to track power commands and possibly provide ancillary services.^{7–12} Some of these designs provide primary response by using inertia response emulation.^{7,8} Another approach is to operate the wind turbine above the optimal tip speed ratio thus reserving kinetic energy.^{9,10} This approach enables the wind turbine to track the power commands and hence this can be used to realize AGC. The use of blade pitch control with or without combined generator torque control has also been explored.^{11,12}

This paper proposes an LPV controller to provide APC. The 2-input, 2-output control architecture builds upon a previous gain-scheduled design,¹³ where collective blade pitch and generator torque are coordinated in order to track power and rotor speed reference commands. The controller has parameter dependence on the wind speed and the power output. The LPV approach, in contrast to the previous ad-hoc gain scheduled design, provides (in theory) guarantees on closed-loop stability and performance.^{14,15} This enables the LPV controller to have a uniform structure and operate smoothly anywhere within the power/wind speed envelope of the turbine. It is also noted that the robustness is an important concern in modern control design for complex systems subject to uncertainties with the nominal model. Therefore, the robustness of this LPV system is analyzed using the theory of integral quadratic constraints (IQCs).^{16–18}

The remainder of the paper is organized as follows. Section II briefly reviews the architecture for APC and the control of LPV systems. The theory of integral quadratic constraints for robust analysis of LPV systems is in Appendix. Section III gives the detailed design process for the LPV controller. Simulation results and robust analysis of the system are presented in Section IV. Finally, conclusions and future work are summarized in Section V.

II. Background

A. Architecture for APC

The traditional turbine control system tries to maximize power production at low wind speeds and keep rated power at high wind speeds to prevent damage of overload to the turbine.^{5,19,20} As shown in Figure 1, the turbine using this control strategy operates on the blue curve of power versus wind speed. However, active power control requires the turbine to adjust its power output according to the command reference from transmission system operator or wind farm. It is important to note that the wind conditions limit the power that can be generated (in steady-state) by the turbine. Specifically, the turbine must operate within the power vs. wind speed envelope below the blue curve. Thus active power control is constrained to power reference commands that are within this envelope. Methods to reserve power and operate within this envelope include de-rating, relative spinning reserves, and absolute spinning reserves.^{10,12,21} Each of these methods corresponds to operation along a specific power vs. wind speed curve that lies within the available power envelope.

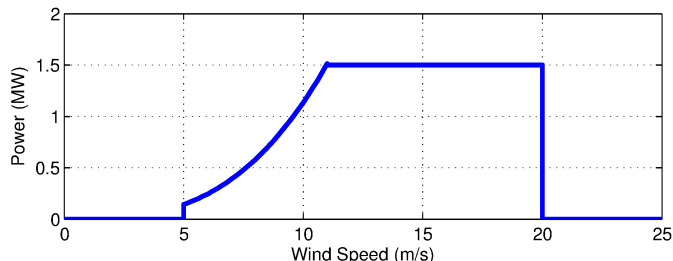


Figure 1. Turbine operating regions.

An approach to realize APC has been proposed in our previous work to operate the turbine anywhere within the power envelope.¹³ It enables de-rating, relative spinning reserves, and absolute spinning reserves as special cases. The control design of this approach is achieved by gain scheduling based on trim power p and wind speed v . However, the gain scheduling is less rigorous than the modern linear parameter varying (LPV) techniques.^{22,23} It is only sufficient for slow variations in the scheduling parameters and there are no formal guarantees on stability and performance. Therefore, a standard LPV design is applied in this paper

to achieve APC. It should be noted that LPV techniques have been applied to the control of wind turbines in some literatures.^{24–26} However, these designs still try to operate the turbine in the traditional way. A brief introduction to the control of LPV systems will be presented in Section II.B.

The way to operate the turbine to achieve APC using LPV builds upon a previous gain-scheduled design¹³ and is now briefly described. To operate at one of the (v, p) trim conditions within the envelope, the turbine must reduce the power coefficient^{5,27} to a new value C_p less than the optimal value C_{p*} by changing the blade pitch angle β and/or the tip speed ratio $\lambda := \frac{R\omega}{v}$, where ω is the rotor speed [rad/s] and R is the radius of the rotor area [m]). As shown in Figure 2, there is a contour of possible values of (λ, β) that achieve any value of $C_p < C_{p*}$. For a given (v, p) trim condition, the controller can be designed to operate at any point on the new C_p contour. To summarize, each (v, p) trim condition corresponds to a desired power coefficient.

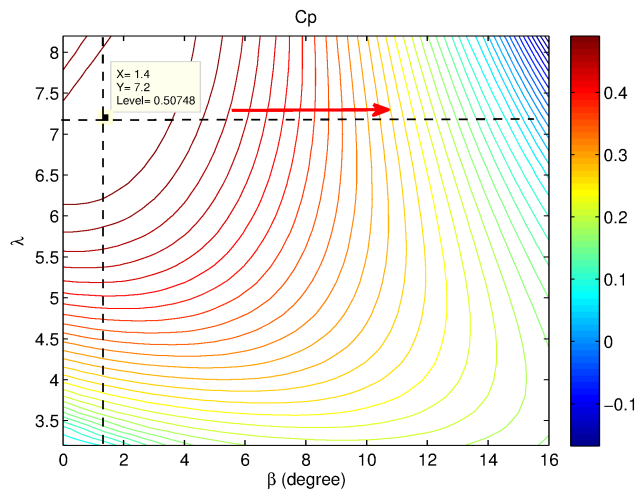


Figure 2. Power coefficient contours for WindPACT 1.5MW Model.

The controller proposed tracks the desired power as follows. In low wind speeds, the controller shifts from (λ_*, β_*) to the desired C_p by increasing to a larger blade pitch $\beta > \beta_*$ while holding tip speed ratio fixed at λ_* . The red arrow in Figure 2 indicates the proposed shift to the desired C_p in low wind speeds. In constant wind conditions, this approach holds desired rotor speed constant (to maintain λ_*) while blade pitch angle is increased to shed extra power according to the desired power command.

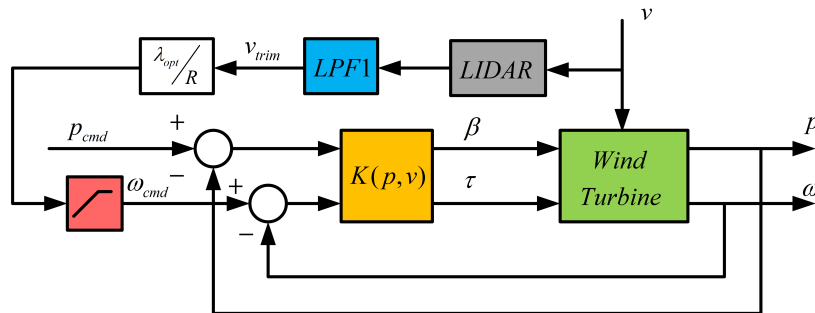


Figure 3. Proposed control strategy for APC.

This strategy can be implemented as the control system structure shown in Figure 3. A 2-input, 2-output control system is used to coordinate the blade pitch and generator torque. The main objective is to track the power reference command p_{cmd} . The rotor speed command ω_{cmd} specifies the desired point on the power coefficient contour. In particular the rotor speed command is defined as follows:

$$\omega_{cmd} = \min \left\{ \frac{v_{trim} \lambda_*}{R}, \omega_{rated} \right\} \quad (1)$$

where ω_{rated} is the rated rotor speed and v_{trim} is an estimate of the effective wind speed. As described above, this rotor speed command attempts to keep the λ at the optimal value λ_* at lower wind speeds. This will cause an increasing rotor speed demand as wind speed increases. At higher wind speeds, the rotor speed command saturates and attempts to maintain the rated rotor speed. It is assumed that an accurate and real time measurement of the wind speed is available. As shown in Figure 3, an estimate of the wind speed could be obtained from a LIDAR.²⁸ Alternatively, an estimate of the effective wind speed could be constructed.²⁹ In either case, the actual wind speed fluctuates and hence low-pass filtering, denoted LPF1 in the figure, is used to smooth out these fluctuations. As mentioned above, this LPV controller is designed to have dependence on trim wind speed v_{trim} and power p_{trim} to ensure the performance in the whole envelope. The low-pass filtered wind speed here also provides the corresponding scheduling parameter for the controller. The other scheduling parameter of power is from low-pass filtered power output measurement which is not shown in Figure 3.

The advantages and drawbacks of this MIMO control architecture have been discussed in.¹³ Compared to the gain scheduled control, the stability can be guaranteed with a standard LPV design here, and it is expected to achieve better performance.

B. Control of LPV Systems

LPV systems are a class of systems whose state space matrices depend on a time-varying parameter vector $\rho : \mathbb{R}^+ \rightarrow \mathbb{R}^{n_\rho}$. An allowable parameter trajectory ρ is a continuously differentiable function of time that is restricted at each point in time to lie in a known compact set $\mathcal{P} \subset \mathbb{R}^{n_\rho}$. In addition, the parameter rates of variation $\dot{\rho} : \mathbb{R}^+ \rightarrow \dot{\mathcal{P}}$ are assumed to lie within a hyperrectangle $\dot{\mathcal{P}}$ defined by

$$\dot{\mathcal{P}} := \{q \in \mathbb{R}^{n_\rho} \mid \underline{v}_i \leq q_i \leq \bar{v}_i, i = 1, \dots, n_\rho\}. \quad (2)$$

The set of admissible trajectories is defined as $\mathcal{A} := \{\rho : \mathbb{R}^+ \rightarrow \mathbb{R}^{n_\rho} : \rho(t) \in \mathcal{P}, \dot{\rho}(t) \in \dot{\mathcal{P}} \forall t \geq 0\}$. The parameter trajectory is said to be rate unbounded if $\dot{\mathcal{P}} = \mathbb{R}^{n_\rho}$.

An n_G^{th} order open loop LPV system G_ρ is defined by

$$\begin{bmatrix} \dot{x} \\ e \\ y \end{bmatrix} = \begin{bmatrix} A(\rho(t)) & B_1(\rho(t)) & B_2(\rho(t)) \\ C_1(\rho(t)) & D_{11}(\rho(t)) & D_{22}(\rho(t)) \\ C_2(\rho(t)) & D_{21}(\rho(t)) & D_{22}(\rho(t)) \end{bmatrix} \begin{bmatrix} x \\ d \\ u \end{bmatrix} \quad (3)$$

where $x \in \mathbb{R}^{n_G}$, $d \in \mathbb{R}^{n_d}$, $e \in \mathbb{R}^{n_e}$, $u \in \mathbb{R}^{n_u}$ and $y \in \mathbb{R}^{n_y}$. The state-space matrices of the LPV system are continuous functions of the parameter. Hence, LPV systems represent a special class of time-varying systems. Throughout the remainder of the paper the explicit dependence on t is suppressed to shorten the notation. Moreover, it is important to emphasize that the state matrices are allowed to have an arbitrary dependence on the parameters.

The performance of an LPV system G_ρ can be specified in terms of its induced L_2 gain from input d to output e . The induced L_2 norm is defined by

$$\|G_\rho\| := \sup_{d \neq 0, d \in L_2, \rho \in \mathcal{A}, x(0)=0} \frac{\|e\|}{\|d\|}. \quad (4)$$

In words, this is the largest input/output gain over all possible inputs $d \in L_2$ and allowable trajectories $\rho \in \mathcal{A}$.

This norm forms the basis for the induced L_2 norm controller synthesis.^{30,31} Consider the open loop LPV system G_ρ as described in Equation 3, the goal is to synthesize an LPV controller K_ρ of the form:

$$\begin{bmatrix} \dot{x}_K \\ u \end{bmatrix} = \begin{bmatrix} A_K(\rho) & B_K(\rho) \\ C_K(\rho) & D_K(\rho) \end{bmatrix} \begin{bmatrix} x_K \\ y \end{bmatrix}. \quad (5)$$

The controller generates the control input u . It has a linear dependence on the measurement y but an arbitrary dependence on the (measurable) parameter ρ . The closed-loop interconnection of G_ρ and K_ρ is given by a lower linear fractional transformation (LFT) and is denoted $\mathcal{F}_l(G_\rho, K_\rho)$. The objective is to

synthesize a controller K_ρ of the specified form to minimize the closed-loop induced L_2 gain from disturbances d to errors e :

$$\min_{K_\rho} \|\mathcal{F}_l(G_\rho, K_\rho)\|. \quad (6)$$

A simple, necessary and sufficient condition does not exist to evaluate the induced L_2 norm of an LPV system. However, there are bounded-real type linear matrix inequality (LMI) conditions that are sufficient to upper bound the gain of an LPV system (Lemma 3.1 in³¹). This sufficient condition forms the basis for the synthesis result.³¹ It should be noted that the synthesis leads to an infinite collection of parameter-dependent linear matrix inequalities (LMIs). A remedy to this problem, which works in many practical examples, is to approximate the set \mathcal{P} by a finite set $\mathcal{P}_{grid} \in \mathcal{P}$ that represents a gridding over \mathcal{P} .

III. LPV Control Design

This section provides details on the LPV approach introduced in Section II.A. The controller is designed for the WindPACT 1.5 MW wind turbine whose model is contained in the FAST simulation package.³² First, an LPV model of the turbine is generated by selecting a gridding set of scheduling parameters that covers the envelope for APC and linearization at each trim point. Next, the control design and realization is described for this grid based LPV model.

A. Model Description

The LPV model of the WindPACT 1.5 MW turbine for APC is chosen to be dependent on trim power and wind speed whose values cover the envelope below the traditional operation power curve, as shown in Figure 4. This will lead to an infinite collection of parameter-dependent LMIs in control synthesis as mentioned in Section II.B. A practical way to deal with this problem is to take a finite gridding set of scheduling parameters and generate the LTI model at each gridding point. The gain scheduling approach in¹³ took 36 points for design. However, the complexity of solving corresponding LMIs in LPV synthesis will be relatively high with so many points. Here, for simplicity, only 9 points are chosen uniformly in increments of $0.6 MW$ in power and $4 m/s$ in wind speed. These 9 trim points are denoted by x's in Figure 4.

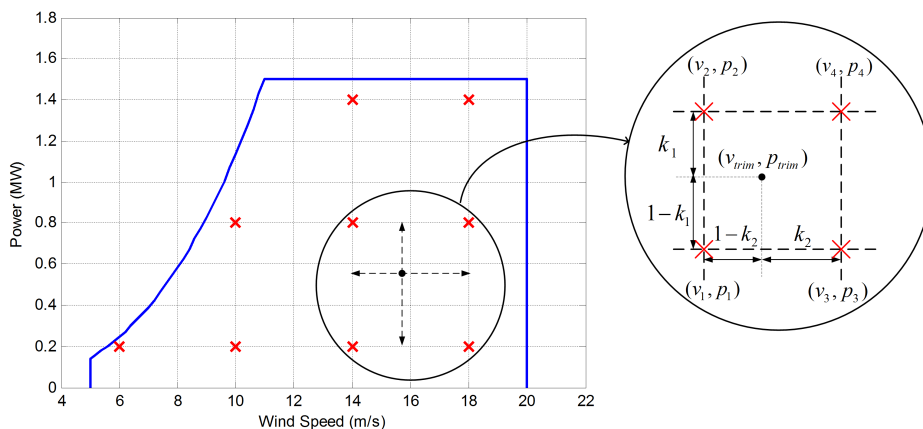


Figure 4. Operation envelope for LPV design.

The LTI model at each trim point is generated by FAST. The FAST simulation package developed by NREL³² is a nonlinear simulation package that is widely used for wind turbine control and analysis. This model includes up to 24 degrees of freedom, including different tower and blade bending modes. FAST models can be linearized at a steady wind speed to obtain a periodic, linear time-varying model. The multi-blade coordinate transformation can then be applied to obtain an approximate LTI model. The resulting LTI models are suitable for advanced control design. However, to simplify the synthesis of the LPV controller this paper uses only 1 degree of freedom which is the rotor position. The corresponding linearized model contains 2 states which are rotor position and speed. To avoid numerical issues in the synthesis step, the state of rotor position is removed. The resulting model with only 1 state left captures the essential aerodynamics

and rotor dynamics of a wind turbine. This model does not contain structural dynamics but it simplifies the design and it is useful for understanding the effectiveness of the proposed APC strategy. Moreover, this model is only used for design but the controller is evaluated using higher fidelity simulations with more degrees of freedom in FAST.

After the trim conditions of power p_0 and wind speed v_0 are selected, trim values can be found for the rotor speed ω_0 , blade pitch angle β_0 and generator torque τ_0 . Let Δ be used to denote the deviation of a variable from its trim condition, e.g. $\Delta\omega := \omega - \omega_0$ denotes the deviation of the rotor speed from the trim operating condition. The LPV model of the turbine is given by state space expression of the form

$$\begin{bmatrix} \dot{x} \\ y \end{bmatrix} = \begin{bmatrix} A(\rho) & B(\rho) \\ C(\rho) & D(\rho) \end{bmatrix} \begin{bmatrix} x \\ u \end{bmatrix} \quad (7)$$

where $x := \Delta\omega$ is the state, $u := \begin{bmatrix} \Delta\beta \\ \Delta\tau \\ \Delta v \end{bmatrix}$ is the vector of inputs, $y := \begin{bmatrix} \Delta p \\ \Delta\omega \end{bmatrix}$ is the vector of outputs, and

$\rho := \begin{bmatrix} v_{trim} \\ p_{trim} \end{bmatrix}$ is the scheduling parameter which is from low-pass filtered wind speed and power output measurements as mentioned in Section II.A.

B. Control Synthesis and Realization

Similar to the tuning in H_∞ control synthesis for LTI systems,^{33,34} different performance weights need to be specified in the induced L_2 control of LPV systems. The augmented system for LPV synthesis is shown in Figure 5. The seven weight functions are chosen to be the same as those used for the gain scheduled design.¹³

Two performance weights, $W_1(s) = 5 \frac{100s + 21}{200s + 0.021}$ and $W_2(s) = 2.5 \frac{100s + 13}{200s + 0.013}$ are used to specify the objectives for power and rotor speed tracking. These weights are chosen to limit the low frequency error with less emphasis on high frequency tracking. Next, $W_3(s) = \frac{2.5}{\pi} \frac{1000s + 11}{s + 21}$ and $W_4(s) = \frac{1}{2000} \frac{100s + 14}{s + 140}$ are two weights used to penalize the actuation of blade pitch angle and generator torque, respectively. Both weights are chosen as high pass filters to penalize high frequency control effort. Finally, the weights $W_5 = 0.2$, $W_6 = 0.4$ and $W_7 = 1.4$ are used to scale the input power command, and rotor speed command, and wind disturbance to values corresponding to 0.2 MW, 0.4 rad/s and 1.4 m/s, respectively. More details about the weights can be found in.¹³

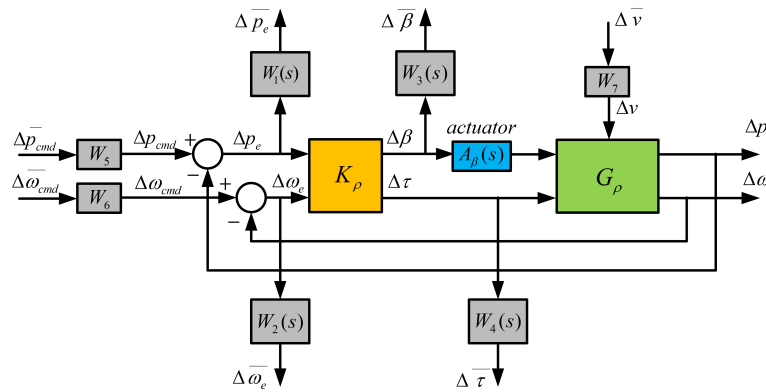


Figure 5. Augmented system for LPV synthesis.

Besides performance weights, ranges of the parameter varying rate need to be specified before synthesis. By selecting the high-pass filtered signal of the trim wind speed v_{trim} , which is shown in Figure 3, the maximum wind acceleration is found to be 0.3 m/s^2 in the average speed of 16 m/s with 5% turbulence. However, to ensure stability of the system in high turbulence, the value is extended to 1 m/s^2 . In practical

application of APC, the reference command of power is expected to change slowly. Therefore, $0.1 MW/s$ is selected for the trim power varying rate. A controller can be designed for a faster rate of variation for desired power if necessary.

The LPV controller is synthesized after solving a finite collection of LMIs. The result is expressed as a set of LTI controllers corresponding to different trim points. Realization of the LPV controller requires linear interpolation of these LTI controllers and the trim values of blade pitch angle β_{trim} and generator torque τ_{trim} . Specifically, the four nearest “grid” trim points $\{v_i, p_i\}_{i=1}^4$ of the current (v_{trim}, p_{trim}) are determined as shown in Figure 4. The fractional distance along each coordinate axis is computed as $k_1 = \frac{p_2 - p_{trim}}{p_2 - p_1}$ and $k_2 = \frac{v_3 - v_{trim}}{v_3 - v_1}$. Finally, the trim blade pitch and generator torque are given by

$$\begin{bmatrix} \beta_{trim} \\ \tau_{trim} \end{bmatrix} = k_2 \left(k_1 \begin{bmatrix} \beta_1 \\ \tau_1 \end{bmatrix} + (1 - k_1) \begin{bmatrix} \beta_2 \\ \tau_2 \end{bmatrix} \right) + (1 - k_2) \left(k_1 \begin{bmatrix} \beta_3 \\ \tau_3 \end{bmatrix} + (1 - k_1) \begin{bmatrix} \beta_4 \\ \tau_4 \end{bmatrix} \right) \quad (8)$$

Some trim conditions near the boundary of the operating area have less than four neighboring “grid” trim points. For conditions with only two neighbors, the interpolation is along a single dimension. For conditions with only three neighbors, i.e. the trim point is in a triangle with vertices of (v_1, p_1) , (v_3, p_3) and (v_4, p_4) , β_{trim} and τ_{trim} are given by

$$\begin{bmatrix} \beta_{trim} \\ \tau_{trim} \end{bmatrix} = k_2 \left(k_1 \begin{bmatrix} \beta_1 \\ \tau_1 \end{bmatrix} + (1 - k_1) \begin{bmatrix} \beta_3 \\ \tau_3 \end{bmatrix} \right) + (1 - k_2) \left(k_1 \begin{bmatrix} \beta_4 \\ \tau_4 \end{bmatrix} + (1 - k_1) \begin{bmatrix} \beta_3 \\ \tau_3 \end{bmatrix} \right) \quad (9)$$

where $k_1 = \frac{p_{trim} - p_3}{p_4 - p_3} + \frac{v_3 - v_{trim}}{v_3 - v_1}$ and $k_2 = \frac{v_3 - v_{trim}}{v_3 - v_1}$. The state-space matrices for the controller, $\begin{bmatrix} A_k & B_k \\ C_k & D_k \end{bmatrix}$ are interpolated in a similar fashion as those given in Equation 8 and 9.

IV. Simulations and Analysis

A. Nominal Performance in Turbulent Wind

The LPV controller designed in Section III was simulated with WindPACT 1.5 MW wind turbine model in FAST. The control design was performed using a 1-state linearized model. However, turbine structural modes were included in all simulation results shown in this section. Specifically, the structural modes for simulation include the first flap-wise blade mode for each blade and the first fore-aft tower bending mode. Including the rotor position, the model has five degrees of freedom. For comparison, the gain scheduled H_∞ controller designed in¹³ was also simulated. However, only nine H_∞ controllers corresponding to trim points in the LPV design were gain scheduled.

In the first simulation, the wind profile contains 5% turbulence at a mean wind speed of $8 m/s$. The power command (red dash-dot line in second subplot of Figure 6) steps from $0.4 MW$ to $0.5 MW$ at $t = 150 s$, then drops to $0.3 MW$ at $t = 300 s$ and finally steps back to $0.4 MW$ at $t = 450 s$. In this wind and power profile, LTI controllers at trim points of $(6 m/s, 0.2 MW)$, $(10 m/s, 0.2 MW)$ and $(10 m/s, 0.8 MW)$ were involved into the linear interpolation for both the LPV and gain scheduled cases. However, the system with the gain scheduled controller was simulated to be unstable under these conditions. A detailed post-analysis revealed that the closed-loop with the original gain-scheduled controller was unstable, i.e. it had a pole in the right half of the complex plane. The LPV controller worked well in this case. This exception demonstrates the stability guarantee for the standard LPV design.

To continue the comparison, the LTI controller at the trim point of $(6 m/s, 0.2 MW)$ was removed for the gain scheduled case. The results are shown in Figure 6 for the gain-scheduled controller (dash green line) and the LPV controller (solid blue line). The subplots are, from top to bottom, the rotor speed, power capture, blade pitch, and generator torque. Since the wind speed is below rated, the rotor speed command specified in Equation 1 is proportional to the low-pass filtered wind speed estimate. This rotor speed command is shown as the dash-dot line in the top subplot. The rotor speed regulation for the LPV controller has smaller error than the gain scheduled one. To evaluate these errors, define the root mean square (RMS) of the rotor

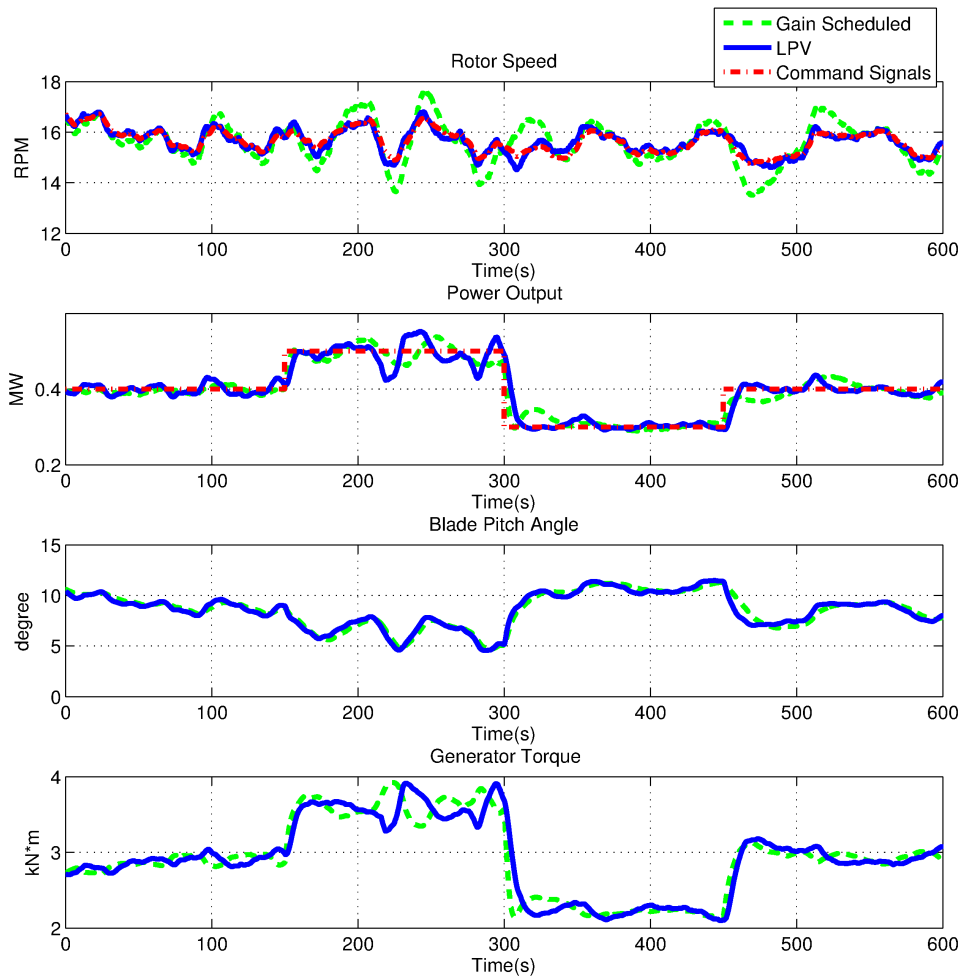


Figure 6. Simulation in below rated turbulent wind.

speed tracking error ω_{RMS} as:

$$\omega_{RMS} = \left(\frac{1}{T} \int_0^T |\omega - \omega_{cmd}|^2 dt \right)^{\frac{1}{2}} \quad (10)$$

T is the simulation time, ω and ω_{cmd} are the rotor speed and the reference. Similarly, the RMS of power tracking error and pitch rate can be defined to evaluate the performance and the pitch actuation. The damage equivalent loads (DEL) are also calculated to evaluate the load reduction performance. All these results are shown in the first part of Table 1 which is labeled by ‘below rated wind’. The LPV controller significantly decreases the rotor speed tracking error in comparison to the original gain-scheduled controller. At the same time, the DEL of the blade root flap-wise bending moment and the tower fore-aft bending moment decrease about 5% (the exact ratio is shown in the parentheses after the value for each item). The DEL of the low speed shaft torque for the LPV controller is slightly higher than the gain scheduled one. However, the RMS power tracking error and pitch rate increase more than 20% for the LPV control. This could be considered as the sacrifice for better rotor speed tracking performance. This trade-off between tracking error, actuator usage, and structural loads will be investigated further in the final version of the paper.

The second simulation was performed at an average wind speed of 16 m/s with 5% turbulence. The results are shown in Figure 7. The power reference command (red dash-dot line in second subplot) steps from 1.1 MW to 1.4 MW at $t = 150$ s, then drops to 0.8 MW at $t = 300$ s and finally steps back to 1.1 MW at $t = 450$ s. The rotor speed command (Equation 1) is held fixed at the rated rotor speed (shown as dashed dot line in top subplot). Compared to the gain scheduled controller, the LPV design shows similar rotor

Table 1. Controller Performance Comparison for Simulations in FAST

| Description | Gain Scheduled | | LPV | Gain Scheduled | | LPV |
|---------------------------------|----------------|--------|--------------------|----------------|--------|--------------------|
| | | | (below rated wind) | | | (above rated wind) |
| Blade Flapwise DEL | 258.6 | 249.0 | (−3.71 %) | 360.8 | 363.6 | (+0.78 %) |
| Tower Fore-after DEL | 3835 | 3610 | (−5.95 %) | 7209 | 6885 | (−4.49 %) |
| Low Speed Shaft DEL | 83.43 | 86.19 | (+3.31 %) | 247.7 | 176.9 | (−28.58 %) |
| RMS Speed Error (RPM) | 0.5047 | 0.1585 | (−68.6 %) | 0.4761 | 0.4635 | (−2.65 %) |
| RMS Power Error (MW) | 0.0213 | 0.0261 | (+22.54 %) | 0.1166 | 0.0456 | (−60.89 %) |
| RMS Pitch Rate (<i>rad/s</i>) | 0.0016 | 0.002 | (+25 %) | 0.006 | 0.0051 | (−15 %) |
| Max Pitch Rate (<i>rad/s</i>) | 0.0092 | 0.0154 | (+67.39 %) | 0.0174 | 0.0176 | (−1.15 %) |

speed regulation performance. The RMS of the tracking errors can be calculated as defined in Equation 19. The second part of Table 1 which is labeled by ‘above rated wind’ verifies this observation. The power tracking and disturbance rejection performance of the LPV design is much better than the gain scheduled controller. The blade pitch actuation is also similar between the two controllers. This is shown in the right column of Table 1. The generator torque of the LPV design varies more smoothly than the gain scheduled controller. This leads to the better power tracking performance as mentioned above and also better load reduction effect on the low speed shaft. Finally, the DEL of the blades and the tower are similar between the LPV controller and the gain scheduled one.

B. Robust Analysis Using IQCs

Robustness is an important concern in modern control design for systems subject to uncertainties with the nominal model. Even though FAST provides a high fidelity simulation environment, the impact of model uncertainty, i.e. the mismatch between the real turbine dynamics and FAST, should be assessed. Due to the nonlinear turbine dynamics, this robustness analysis requires tools that move beyond those available for traditional LTI analysis. Recent developments in the theory of IQCs^{16–18} provide a general framework for robust analysis of LPV systems. Therefore, robustness of the LPV controller designed in this paper will be evaluated using the theoretical results introduced in Appendix.

For simplicity, a multiplicative norm bounded uncertain block Δ is inserted to the input channel of blade pitch, as shown in Figure 8. The norm of the uncertainty is assumed to be less than a positive scalar b , i.e. $\|\Delta\| \leq b$. The uncertainty is described by the integral quadratic constraints (Ψ, M) with $\Psi = I_2$ and $M = \begin{bmatrix} 1 & 0 \\ 0 & -b^{-2} \end{bmatrix}$. Here G_ρ and K_ρ represent the LPV model and controller of the turbine described by LTI state space models at nine gridding parameters as shown in Section III. The induced L_2 gain from reference commands and wind disturbance $\begin{bmatrix} \Delta p_{cmd} \\ \Delta \omega_{cmd} \\ \Delta v \end{bmatrix}$ to the outputs $\begin{bmatrix} \Delta p \\ \Delta \omega_{cmd} \end{bmatrix}$ is used as performance measurement.

The worst case gains of the LPV system corresponding to different values of the uncertainty bound b are calculated under two set of parameter varying rates. In the first set, the bound of wind acceleration, which is denoted as $\dot{\rho}_1$ is $0.1 m/s^2$; the bound of power varying rate, which is denoted as $\dot{\rho}_2$, is $0.001 MW/s$. In the second set, the corresponding values are $0.2 m/s^2$ and $0.002 MW/s$. Both cases assume the Lyapunov matrix $P(\rho)$ has affine dependence on parameters, i.e. $P(\rho) = P_0 + \rho_1 P_{11} + \rho_2 P_{12}$, where P_0 , P_{11} and P_{12} are constant matrices. The parameter rate of power is chosen much lower than the original design in both cases here for some numerical issues. As comparison, the LTI worst case gain of the system in the presence of uncertainty is calculated at some frozen parameters. The results are shown in Figure 9. The worst case gain without uncertainty is 13.5 for the first set of parameter varying rates. The corresponding value is 16.7 for the second set. The LTI worst case gain is only 1.5. As the norm bound b of the uncertainty increases, the value of γ increases in each of the three cases. The γ for slower parameter varying rates in the first case is always lower than the second one. The γ for the LTI case is much lower than both of the parameter varying cases. The results show that the robustness performance of LPV system is worse than the frozen LTI case and will deteriorate as the bound of parameter varying rates increase. This makes sense because the frozen LTI system could be recognized as the LPV system with parameter varying rates equal to 0. It should be noted that the γ calculated using the proposed method in Appendix only provides an upper bound of the worst case gain of the LPV system because of the sufficient condition in Theorem 1. The conservativeness

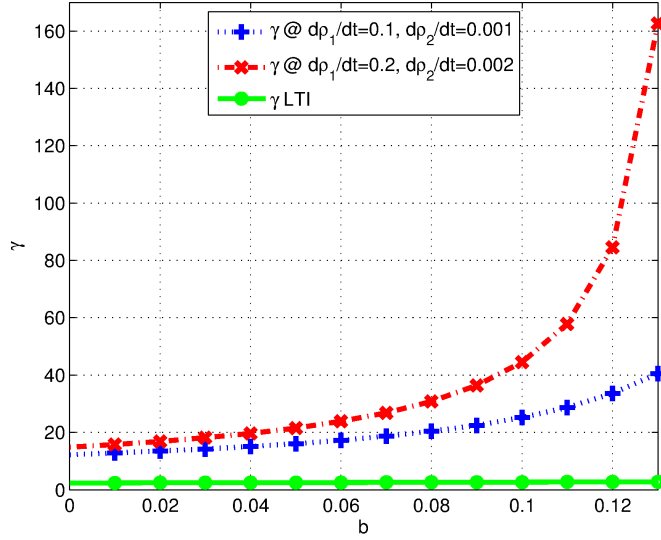


Figure 9. Worst case gain of the system with uncertain β .

output whose range cover the turbine operation envelope for APC. Compared to the gain scheduled approach in the previous design, a standard LPV design ensures the stability and performance of the system. This is certified by simulations on FAST and post statistical analysis. Moreover, the robustness of the LPV system was evaluated using IQCs. However, several aspects of the design need further consideration. These include the actuator saturation of blade pitch in low wind speed and high power command, tuning on the LPV design, simulations with more realistic wind and power profiles and more results and interpretations on robust analysis of the system.

Appendix

IQCs are used to model the uncertain and/or nonlinear components and provide a general framework for robustness analysis.¹⁶ While the frequency-domain stability condition in¹⁶ applies only for uncertain LTI systems, a time-domain interpretation and the derived dissipation inequality condition could be used for robust analysis of uncertain LPV systems.¹⁸

An IQC is defined by a symmetric matrix $M = M^T \in \mathbb{R}^{n_z \times n_z}$ and a stable linear system $\Psi \in \mathbb{RH}_{\infty}^{n_z \times (n_v + n_w)}$. Ψ is denoted as

$$\begin{bmatrix} \dot{x}_{\psi}(t) \\ z(t) \end{bmatrix} = \begin{bmatrix} A_{\psi} & B_{\psi 1} & B_{\psi 2} \\ C_{\psi} & D_{\psi 1} & D_{\psi 2} \end{bmatrix} \begin{bmatrix} x_{\psi}(t) \\ v(t) \\ w(t) \end{bmatrix} \quad (11)$$

The initial condition for Ψ is always taken as $x_{\psi}(0) = 0$.

Definition 1 A bounded, causal operator $\Delta : L_{2e}^{n_v} \rightarrow L_{2e}^{n_w}$ satisfies an IQC defined by (Ψ, M) if the following inequality holds for all $v \in L_2^{n_v}[0, \infty)$, $w = \Delta(v)$ and $T \geq 0$:

$$\int_0^T z(t)^T M z(t) dt \geq 0 \quad (12)$$

where z is the output of the linear system Ψ as defined in Equation 11. The notation $\Delta \in \text{IQC}(\Psi, M)$ is used if Δ satisfies the IQC defined by (Ψ, M) .

Figure 10 provides a graphical interpretation of the IQC. The input and output signals of Δ are filtered through Ψ . If $\Delta \in \text{IQC}(\Psi, M)$ then the output signal z satisfies the (time-domain) constraint in Equation 12 for any finite-horizon $T \geq 0$. A simple example is provided below to connect this terminology to standard results used in robust control.

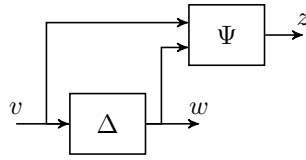


Figure 10. Graphical interpretation of the IQC

Example 1 Consider a causal (SISO) operator Δ that satisfies the bound $\|\Delta\| \leq b$. The norm bound on Δ implies that $\|w\| \leq b\|v\|$ for any input/output pair $v \in L_2$ and $w = \Delta(v)$. This constraint on (v, w) can be expressed as the following infinite-horizon inequality:

$$\int_0^\infty \begin{bmatrix} v(t) \\ w(t) \end{bmatrix}^T \begin{bmatrix} 1 & 0 \\ 0 & -b^{-2} \end{bmatrix} \begin{bmatrix} v(t) \\ w(t) \end{bmatrix} dt \geq 0 \quad (13)$$

It can be shown that the causality of Δ implies the inequality involving (v, w) holds over all finite horizons $T \geq 0$:

$$\int_0^T \begin{bmatrix} v(t) \\ w(t) \end{bmatrix}^T \begin{bmatrix} 1 & 0 \\ 0 & -b^{-2} \end{bmatrix} \begin{bmatrix} v(t) \\ w(t) \end{bmatrix} dt \geq 0$$

A detailed proof is given in.¹⁸ The final conclusion is that $\|\Delta\| \leq b$ satisfies the IQC defined by (Ψ, M) with $\Psi := I_2$ and $M := \begin{bmatrix} 1 & 0 \\ 0 & -b^{-2} \end{bmatrix}$. In this example Ψ contains no dynamics and hence $z = [v^T, w^T]^T$.

An uncertain LPV system is described by the interconnection of an LPV system G_ρ and an uncertainty Δ , as depicted in Figure 11. This interconnection represents an upper LFT denoted $\mathcal{F}_u(G_\rho, \Delta)$. The filter Ψ has been included in Figure 11 as it is used for the analysis.

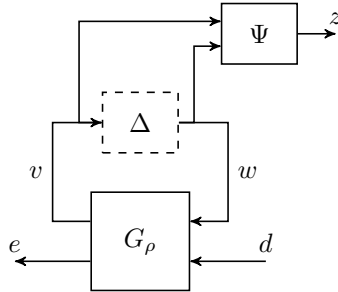


Figure 11. Analysis Interconnection

The dynamics of the analysis interconnection in Figure 11 are described by $w = \Delta(v)$ and

$$\begin{bmatrix} \dot{x} \\ z \\ e \end{bmatrix} = \begin{bmatrix} A(\rho) & B_1(\rho) & B_2(\rho) \\ C_1(\rho) & D_{11}(\rho) & D_{12}(\rho) \\ C_2(\rho) & D_{21}(\rho) & D_{22}(\rho) \end{bmatrix} \begin{bmatrix} x \\ w \\ d \end{bmatrix} \quad (14)$$

where the state vector is $x = [x_G; x_\psi] \in \mathbb{R}^{n_G+n_\psi}$ with x_G and x_ψ being the state vectors of the LPV system G_ρ and the filter Ψ respectively. The uncertainty Δ is shown in the dashed box to signify that it is removed for the analysis. The signal w is treated as an external signal subject to the constraint in Equation 12. This effectively replaces the precise relation $w = \Delta(v)$ with the quadratic constraint on z .

The next theorem provides a (sufficient) dissipation-inequality condition to upper bound of the worst case L_2 gain of $\mathcal{F}_u(G_\rho, \Delta)$.¹⁸ This sufficient condition uses a quadratic storage function that is defined using a parameter-dependent matrix $P : \mathcal{P} \rightarrow \mathbb{S}^{n_G+n_\psi}$. It is assumed that P is a continuously differentiable

function of the parameter ρ . In order to shorten the notation, a differential operator $\partial P : \mathcal{P} \times \dot{\mathcal{P}} \rightarrow \mathbb{S}^{n_G+n_\psi}$ is introduced as in.³⁵ ∂P is defined as:

$$\partial P(\rho, \dot{\rho}) := \sum_{i=1}^{n_\rho} \frac{\partial P(\rho)}{\partial \rho_i} \dot{\rho}_i \quad (15)$$

Theorem 1 *Assume $\mathcal{F}_u(G_\rho, \Delta)$ is well posed for all $\Delta \in IQC(\Psi, M)$. Then the worst-case gain of $\mathcal{F}_u(G_\rho, \Delta)$ is $\leq \gamma$ if there exists a continuous differentiable $P \in \mathcal{P} \rightarrow \mathbb{S}^{n_G+n_\psi}$ and a scalar $\lambda \geq 0$ such that $P \geq 0$ and $\forall(\rho, \dot{\rho}) \in \mathcal{P} \times \dot{\mathcal{P}}$*

$$\begin{bmatrix} PA + A^T P + \partial P & PB_1 & PB_2 \\ B_1^T P & 0 & 0 \\ B_2^T P & 0 & -I \end{bmatrix} + \lambda \begin{bmatrix} C_1^T \\ D_{11}^T \\ D_{12}^T \end{bmatrix} M \begin{bmatrix} C_1 & D_{11} & D_{12} \end{bmatrix} + \frac{1}{\gamma^2} \begin{bmatrix} C_2^T \\ D_{21}^T \\ D_{22}^T \end{bmatrix} \begin{bmatrix} C_2 & D_{21} & D_{22} \end{bmatrix} < 0 \quad (16)$$

In Equation 16 the dependence of the state matrices on ρ and $\dot{\rho}$ has been omitted.

For simplicity, details of the proof are ignored here but could be found in.¹⁸

Acknowledgments

This work was supported by the National Science Foundation under Grant No. NSF-CMMI-1254129 entitled "CAREER: Probabilistic Tools for High Reliability Monitoring and Control of Wind Farms." This work was also supported by the University of Minnesota Institute on the Environment, IREE Grants No. RS-0039-09 and RL-0011-13. Any opinions, findings, and conclusions or recommendations expressed in this material are those of the authors and do not necessarily reflect the views of the National Science Foundation.

References

- ¹"World Wind Energy Report 2011," *Proceedings of the 11 th World Energy Conference*, World Wind Energy Association, Bonn, Germany, 2012.
- ²Crabtree, G., Misewich, J., Ambrosio, R., Clay, K., DeMartini, P., James, R., Lauby, M., Mohta, V., Moura, J., Sauer, P., et al., "Integrating Renewable Electricity on the Grid," *AIP Conference Proceedings-American Institute of Physics*, Vol. 1401, 2011, p. 387.
- ³Aho, J., Bucksan, A., Laks, J., Fleming, P., Jeong, Y., Dunne, F., Churchfield, M., Pao, L., and Johnson, K., "A Tutorial of Wind Turbine Control for Supporting Grid Frequency through Active Power Control," *Proceedings of American Control Conference*, IEEE, 2012, pp. 3120–3131.
- ⁴Rebours, Y., Kirschen, D., Trotignon, M., and Rossignol, S., "A Survey of Frequency and Voltage Control Ancillary Services-Part I: Technical Features," *IEEE Transactions on Power Systems*, Vol. 22, No. 1, 2007, pp. 350–357.
- ⁵Burton, T., Sharpe, D., Jenkins, N., and Bossanyi, E., *Wind Energy Handbook*, John Wiley & Sons, 1st ed., 2001.
- ⁶Greedy, L., "Review of electrical drive-train topologies," *Project UpWind, Mekelweg, the Netherlands and Aalborg East, Denmark, Tech. Rep.*, 2007.
- ⁷Nelson, R. J., "Frequency-Responsive Wind Turbine Output Control," 2011, U.S. Patent 0 001 318.
- ⁸Keung, P.-K., Li, P., Banakar, H., and Ooi, B. T., "Kinetic Energy of Wind Turbine Generators for System Frequency Support," *IEEE Transactions on Power Systems*, Vol. 24, No. 1, 2009, pp. 279–287.
- ⁹Juankorena, X., Esandi, I., López, J., and Marroyo, L., "Method to Enable Variable Speed Wind Turbine Primary Regulation," *International Conference on Power Engineering, Energy and Electrical Drives, 2009*, IEEE, 2009, pp. 495–500.
- ¹⁰Aho, J., Bucksan, A., Pao, L., and Fleming, P., "An Active Power Control System for Wind Turbines Capable of Primary and Secondary Frequency Control for Supporting Grid Reliability," *51st AIAA Aerospace Sciences Meeting including the New Horizons Forum and Aerospace Exposition*, 2013, pp. AIAA 2013–0456.
- ¹¹Acedo Sanchez, J., Carcar, M., Lusarreta, M., Perez Barbachano, J., Simon Segura, S., Sole Lopez, D., Zabaleta Maeztu, M., Marroyo Palomo, L., Lopez Taberna, J., et al., "Method of Operation of A Wind Turbine to Guarantee Primary or Secondary Regulation in An Electric Grid," 2011, U.S. Patent 0 057 445.
- ¹²Jeong, Y., Johnson, K., and Fleming, P., "Comparison and testing of power reserve control strategies for grid-connected wind turbines," *Wind Energy*, 2013.
- ¹³Wang, S. and Seiler, P., "Gain Scheduled Active Power Control for Wind Turbines," *AIAA Atmospheric Flight Mechanics Conference*, 2014.
- ¹⁴Apkarian, P., Gahinet, P., and Becker, G., "Self-scheduled H_∞ Control of Linear Parameter-varying Systems: a Design Examples," *Automatica*, Vol. 31, No. 9, 1995, pp. 1251–1261.
- ¹⁵Bobanac, V., Jelavić, M., and Perić, N., "Linear Parameter Varying Approach to Wind Turbine Control," *14th International Power Electronics and Motion Control Conference*, 2010, pp. T12–60–T12–67.
- ¹⁶Megretski, A. and Rantzer, A., "System Analysis via Integral Quadratic Constraints," *IEEE Trans. on Automatic Control*, Vol. 42, 1997, pp. 819–830.

- ¹⁷Seiler, P., “Nonlinear Stability Analysis with Dissipation Inequalities and Integral Quadratic Constraints,” *Submitted to the IEEE Trans. on Automatic Control*, 2013.
- ¹⁸Pfifer, H. and Seiler, P., “Robustness Analysis of Linear Parameter Varying Systems Using Integral Quadratic Constraints,” *American Control Conference*, 2014.
- ¹⁹Bossanyi, E., “The design of closed loop controllers for wind turbines,” *Wind Energy*, Vol. 3, 2000, pp. 149–163.
- ²⁰Laks, J., Pao, L., and Wright, A., “Control of Wind Turbines: Past, Present, and Future,” *Proceedings of American Control Conference*, 2009, pp. 2096–2103.
- ²¹Tarnowski, G., Kjær, P., Dalsgaard, S., and Nyborg, A., “Regulation and Frequency Response Service Capability of Modern Wind Power Plants,” *Proceedings of IEEE Power and Energy Society General Meeting*, 2010, pp. 1–8.
- ²²Packard, A., “Gain Scheduling via Linear Fractional Transformations,” *Systems and Control Letters*, Vol. 22, 1994, pp. 79–92.
- ²³Apkarian, P. and Gahinet, P., “A Convex Characterization of Gain-scheduled H_∞ Controllers,” *IEEE Transactions on Automatic Control*, Vol. 40, No. 5, 1995, pp. 853–864.
- ²⁴Bobanac, V., Jelavić, M., and Perić, N., “Linear Parameter Varying Approach to Wind Turbine Control,” *14th International Power Electronics and Motion Control Conference*, 2010, pp. T12–60–T12–67.
- ²⁵Bianchi, F., Mantz, R., and Christiansen, C., “Control of variable-speed wind turbines by LPV gain scheduling,” *Wind Energy*, Vol. 7, No. 1, 2004, pp. 1–8.
- ²⁶Bianchi, F., Mantz, R., and Christiansen, C., “Gain scheduling control of variable-speed wind energy conversion systems using quasi-LPV models,” *Control Engineering Practice*, Vol. 13, No. 2, 2005, pp. 247–255.
- ²⁷Manwell, J., McGowan, J., and Rogers, A., *Wind Energy Explained: Theory, Design, and Application*, Wiley, 2010.
- ²⁸Mikkelsen, T., Hansen, K., Angelou, N., Sjöholm, M., Harris, M., Hadley, P., Scullion, R., Ellis, G., and Vives, G., “Lidar wind speed measurements from a rotating spinner,” *Proc. European Wind Energy Conference, Warsaw, Poland*, 2010.
- ²⁹Knudsen, T., Bak, T., and Soltani, M., “Prediction models for wind speed at turbine locations in a wind farm,” *Wind Energy*, Vol. 14, No. 7, 2011, pp. 877–894.
- ³⁰Wu, F., *Control of Linear Parameter Varying Systems*, Ph.D. thesis, University of California, Berkeley, 1995.
- ³¹Wu, F., Yang, X. H., Packard, A., and Becker, G., “Induced \mathcal{L}_2 norm control for LPV systems with bounded parameter variation rates,” *International Journal of Robust and Nonlinear Control*, Vol. 6, 1996, pp. 983–998.
- ³²Jonkman, J. and Buhl, M., *FAST User’s Guide*, National Renewable Energy Laboratory, Golden, Colorado, 2005.
- ³³Zhou, K., Doyle, J. C., and Glover, K., *Robust and Optimal Control, 1st Edition*, Prentice Hall, 1996.
- ³⁴Skogestad, S. and Postlethwaite, I., *Multivariable Feedback Control*, John Wiley and Sons Ltd., 2007.
- ³⁵Scherer, C. and Wieland, S., “Linear Matrix Inequalities in Control,” Lecture notes for a course of the dutch institute of systems and control, Delft University of Technology, 2004.